Cancer Nano (2013) 4:57–71
DOI 10.1007/s12645-013-0037-4

ORIGINAL PAPER

Encapsulation of exemestane in polycaprolactone nanoparticles: optimization, characterization, and release kinetics

Abhinesh Kumar · Krutika Sawant

Received: 5 November 2012 / Revised: 21 March 2013 / Accepted: 25 March 2013 / Published online: 25 April 2013

Abstract This study was aimed at developing a polymeric drug delivery system for a steroidal aromatase inhibitor, exemestane (exe) intended for sustained targeted delivery of drug through intravenous route. Carboxylated polycaprolactone (cPCL) was synthesized by ring opening polymerization of caprolactone. Exe-loaded cPCL nanoparticles (NPs) were prepared by interfacial deposition of preformed polymer and characterized. A 3-factor, 3-level Box–Behnken design was used to derive a second-order polynomial equation and construct contour and response plots for maximized response of percentage drug entrapment (PDE) with constraints on particle size (PS). The independent variables selected were ratio of exe/cPCL, amount of cPCL, and volume of organic phase. Polymerization of caprolactone to cPCL was confirmed by Fourier transform infrared (FTIR) and gel permeation chromatography. The prepared NPs were evaluated for differential scanning calorimetry (DSC), transmission electron microscopy (TEM), and in vitro release studies. Optimum formulation based on desirability (1.0) exhibited PDE of 83.96 % and PS of 180.5 nm. Check point analysis confirmed the role of the derived polynomial equation and contour plots in predicting the responses. Zeta potential of optimized formulation was −33.8±2.1 mV. DSC studies confirmed the absence of any interaction between drug and polymer. TEM image showed non-aggregated and spherical shaped NPs. Drug release from NPs showed sustained release and followed Korsmeyer–Peppas model, indicating Fickian drug release. Thus, preparation of exe-loaded cPCL NPs with high PDE and desired PS suitable for providing passive targeting could be statistically optimized using Box–Behnken design.

Keywords Exemestane · Polycaprolactone · Nanoparticles · Box–Behnken design

Abbreviations

Exe	Exemestane
PCL	Polycaprolactone
cPCL	Carboxylated polycaprolactone
NPs	Nanoparticles
BBD	Box–Behnken design
DSC	Differential scanning calorimetry
TEM	Transmission electron microscopy
PDE	Percentage drug entrapment
PS	Particle size
FM	Full model
RM	Reduced model

1 Background

Breast cancer is the leading cause of death among women, with one million new cases in the world each year (McPherson et al. 2000), out of which one third are reported to be hormone dependent (Henderson and Canellos 1980; Theobald 2000). Growth of breast cancer cells is often estrogen dependent. Continuous estrogen suppression in patients with hormone-sensitive breast cancer prevents proliferation of tumor. Aromatase is the key enzyme that converts androgens to estrogens both in pre- and postmenopausal women (Lonning 1998; Strassmer-Weippl and Goss 2003). Exemestane (exe) is a third generation, potent irreversible type I steroidal aromatase inhibitor approved by the Food and Drug Administration

Electronic supplementary material The online version of this article (doi:10.1007/s12645-013-0037-4) contains supplementary material, which is available to authorized users.

A. Kumar · K. Sawant (✉)
Drug Delivery Research Laboratory, TIFAC Center of Relevance and Excellence in NDDS, Pharmacy Department, The Maharaja Sayajirao University of Baroda, Shri G.H. Patel Pharmacy Building, Fatehgunj, Vadodara-390002, Gujarat, India
e-mail: dr_krutikasawant@rediffmail.com

for the treatment of breast cancer (Johannessen et al. 1997). It acts as a false substrate for the aromatase enzyme and is processed to an intermediate that binds irreversibly to the active site of the enzyme causing its inactivation, an effect also known as suicide inhibition (Dowsett 1998). Although treatment with orally administered exe has been shown to be well tolerated by patients, the most common adverse events consist of hot flashes, nausea, fatigue, dizziness, increased sweating, headache, body weight change, vaginal dryness, arthralgias, and myalgias (Scott and Wiseman 1999; Clemett and Lamb 2000). The problem with the oral delivery of exe is its inability to target the tumor site. This problem can be overcome by employing delivery systems capable of providing targeted drug delivery. Poly(lactic-co-glycolic acid) (PLGA) nanoparticles (NPs) are already reported to provide passive targeting of anticancer drugs to tumor site (Yallapu et al. 2010; Fonseca et al. 2002).

Polymeric NPs with a diameter of less than 200 nm are one of the carrier systems used for passive targeting and sustained release of drug. NPs regroup both nanocapsules and nanospheres. Polycaprolactone (PCL) is a biodegradable polyester and is prepared by ring opening polymerization of ε-caprolactone. PCL is degraded by hydrolysis of its ester linkages in physiological conditions and has therefore received a great deal of attention for use as a biomaterial for sustained release drug delivery systems (Lam et al. 2008; Aberturas et al. 2011). Different methods reported for preparing NPs using biodegradable polymers include monomer polymerization, interfacial deposition, salting out, nanoprecipitation, emulsification solvent evaporation, etc. (Quintanar-Guerrero et al. 1998). Interfacial deposition of preformed polymer technique is based upon interfacial deposition of a polymer followed by diffusion of a semi-polar and miscible solvent in aqueous medium containing surfactant (Fessi et al. 1989; Barichello et al. 1999). Moraes et al. used this method for preparation of PLGA nanocapsules with particle size (PS) of 123 nm and 69 % drug loading (Moraes et al. 2009). Formulation of NPs by this method involves many important factors which contribute to the outcome of experiment in terms of drug entrapment and PS. Different process variables include stirring speed, temperature, rate of addition of organic phase to aqueous phase, etc. Different formulation variables include drug/polymer ratio, concentration of polymer in organic phase, surfactants, surfactant concentration, volume of aqueous and organic phase, organic solvents, etc.

Optimization by changing one-variable-at-a-time is a complex method to evaluate the effects of different variables on an experimental outcome. This approach assesses one variable at a time instead of all simultaneously. The method is time consuming, expensive, and often leads to misinterpretation of results when interactions between different components are present. Another approach is to accurately evaluate the impact of the independent variables on the dependent variables by varying all the important factors simultaneously in a systematic manner. This approach is known as response surface methodology (RSM). RSM is a statistical technique which can address the present scenario and can be used to establish relationships between several independent variables and one or more dependent variables (Myer and Montogomery 2002; Ray et al. 2009). RSM optimizes multiple variables by systematic variation of all variables in a well-designed experiment with a minimum number of experiments. The RSM optimization process involves the following steps: (1) performing statistically designed experiments, (2) estimating the coefficients of a mathematical model using regression analysis technique, and (3) predicting the response and checking the adequacy of the model. Among the available statistical design methods, a full factorial design (FFD) involves a large number of experiments for accurately predicting the response. At the same time, it is often considered unpractical due to its requirement of more number of experiments as compared with other designs (Box et al. 1978; Myer et al. 1989). Fractional factorial design lacks the ability to accurately predict all positions of the factor space that are equidistant from the centre (rotatability). Based upon the desirable features of orthogonality and rotatability, central composite design (CCD), and Box–Behnken design (BBD) are commonly chosen for the purpose of response optimization (Bae and Shoda 2005; Ray 2006). BBD was successfully used by Rahman et al. for optimization of risperidone-loaded solid lipid NPs (Rahman et al. 2010).

The BBD was specifically selected since it requires fewer runs than three-factor, three-level FFD and CCD when three or more variables are involved. This cubic design is characterized by a set of points lying at the midpoint of each edge and a replicate centre point of the multidimensional cube (George Box 1960). The BBD technique is a three-level design based upon the combination of two-level factorial designs and incomplete block designs. BBD is a spherical design with excellent predictability within the spherical design space. Compared with the CCD method, the BBD technique is considered as the most suitable for evaluating quadratic response surfaces particularly in cases when prediction of response at the extreme level is not the goal of the model. In addition, the BBD technique is rotatable or nearly rotatable regardless of the number of factors under consideration (Myer and Montogomery 2002; Bae and Shoda 2005; Ray 2006). However, it is a very time-consuming method. Hence, deriving a quantitative mathematical relationship between the variables to evaluate its effect on dependent variables is of utmost importance (Seth and Misra 2002; Mehta et al. 2007).

In the present study, exe-loaded carboxylated polycaprolactone (cPCL) NPs were prepared by interfacial deposition of

preformed polymer technique and optimized using three-factor, three-level Box–Behnken design. The prepared NPs were characterized for percentage drug entrapment (PDE), particle size, zeta potential, compatibility, morphology, in vitro drug release studies, and release kinetics. It was hypothesized that cPCL-based NPs of exe would be capable of passive targeting to the tumor due to PS of less than 200 nm and provide sustained drug release. This would help to improve clinical utility, decrease the dose and frequency of dosing, reduce side effects, and improve therapeutic efficacy of exe in cancer management.

2 Materials and methods

2.1 Materials

Exe was obtained as a gift sample from Sun Pharma Advanced Research Centre, Vadodara, India. Poloxamer 188 was a gift sample from BASF, Ludwigshafen, Germany. Capric/caprylic triglyceride (Capmul MCM, C8) was obtained as gift sample from Abitec Corporation, Janesville, WI. Caprolactone monomer was purchased from Sigma-Aldrich, Mumbai, India. All other chemicals were of analytical grade and obtained commercially.

2.2 Synthesis of cPCL

Synthesis of carboxylated PCL was carried out by ring opening polymerization of caprolactone monomer in presence of succinic acid as reported by Zhang et al. (1994) with some modifications. Reaction was carried out at room temperature in presence of tertiary butoxide (4 g) for 24 h instead of heating reaction mixture at 225 °C for 3 h. Polymerization was carried out in a flask sealed with a ball filled with nitrogen. The reactant mixture of succinic acid (23.5 mg) and caprolactone (3.65 g) was added to about 15 ml of dichloromethane in the flask for initiation of polymerization reaction. The reaction was catalyzed using tertiary butoxide (4 g). The reaction was allowed to continue for 24 h. The reaction mixture was precipitated in ice-cold water and precipitates were dissolved in acetone for re-precipitation and purification to remove excess succinic acid. Each reaction step as well as purification step was monitored by TLC using 100 % ethyl acetate as a mobile phase and iodine as a spotting reagent. The reaction was considered to be complete when there was absence of spots for caprolactone monomer and succinic acid from the reaction mixture.

2.3 Fourier transform infrared spectroscopy

The sample (2 mg) was finely grounded with purified potassium bromide (200 mg; to remove scattering effects from large crystals). This powder mixture was then pressed in a mechanical die press to form a pellet. These pellets were scanned and spectra were recorded on Fourier transform infrared (FTIR; Bruker Corporation, Billerica, MA). The scanning range was 400–4,000 cm^{-1} with the resolution of 2 cm^{-1}.

2.4 Molecular weight determination

Gel permeation chromatography (GPC) was carried out to determine the molecular weight of the formed polymer (Behan et al. 2001). A GPC (Perkin Elmer, Series 200, Shelton, CT) equipped with a Waters 510 pump, 50°, 10–3°, and 10–4°A Phenogel columns serially set (Phenomenex, Torrance, CA) and a Waters 410 differential refractometer were used. The mobile phase was tetrahydrofuran (THF) at a flow rate of 1.0 ml/min; 50 μl of a 2 % polymer solution in THF was injected into the system, and size exclusion chromatogram was recorded.

2.5 Preparation of exe-loaded cPCL NPs

cPCL NPs loaded with exe were prepared by interfacial deposition of preformed polymer (Fessi et al. 1989). Exe (5 mg) was dissolved in oil (400 μl capric/caprylic triglyceride mixture) and added to acetone (8 ml) in which cPCL (100 mg) was dissolved along with sorbitan monooleate (Span 60, 0.05 ml), under moderate magnetic stirring. This solution was then added to an aqueous phase (40 ml distilled water) containing Poloxamer 188 (0.5 %) with continuous stirring on magnetic stirrer at room temperature. Stirring was continued for 3–4 h to allow complete evaporation of organic solvent. The NPs suspension was centrifuged at 50,000×*g* for 30 min at 4 °C (3K30, Sigma Centrifuge, Osterode, Germany), supernatant was alienated, nanoparticulate pellet was re-dispersed in water (10 ml) and lyophilized (Heto Drywinner, Allerod, Denmark) using sucrose as cryoprotectant (NPs (one part) and cryoprotectant (two parts)). Empty NPs were prepared by the method described above with the exception of adding exe. Based on preliminary experiments, variables like drug/polymer ratio (X_1), amount of polymer (X_2), and volume of organic phase (X_3) were selected as independent variables and PDE and PS were taken as dependent variables. Effect of independent variables on dependent variables was studied using 3×3 Box–Behnken design.

2.6 Lyophilization and optimization of cryoprotectant

Lyophilization is the process in which freeze-drying is done to remove solvent from the formulation and therefore improve its stability upon storage. The process of freeze drying is stressful and hence a cryoprotectant is added in the process, which also helps in re-dispersibility of the freeze-dried NPs in a suitable solvent (Chacon et al. 1999). One of the main challenges

during the freeze-drying process is preserving or rather increasing the re-dispersibility of the NPs upon reconstitution with distilled water or buffered saline. Cryoprotectants are generally added to the NPs prior to the drying step and also act as re-dispersants. Cryoprotectants such as trehalose, sucrose, and mannitol can be used to increase the physical stability of NPs during the freeze-drying process (Paolicelli et al. 2010). In the present study, trehalose, sucrose, and mannitol were investigated in different ratios and change in PS upon re-dispersion was observed. Nanoparticulate suspension (2 ml) was dispensed in 10 ml semi-stoppered glass vials with rubber closures and frozen for 24 h at −60 °C. Thereafter, the vials were lyophilized (Heto Drywinner, Allerod, Denmark) using different cryoprotectants like trehalose, sucrose, and mannitol in different concentrations. Finally, vials were sealed under anhydrous conditions and stored until being re-hydrated. Lyophilized NPs were re-dispersed in exactly the same volume of distilled water as before lyophilization. NP suspension was subjected to PS measurement as described earlier. Ratio of final PS (S_f) and initial PS (S_i) was calculated to finalize the suitable cryoprotectant based on lowest S_f/S_i ratio.

2.7 HPLC analysis

Quantitative estimation of exe was done by HPLC as reported by Breda et al. with slight modification in mobile phase which consisted of a filtered and degassed mixture of acetonitrile/0.02 M phosphate buffer (pH 4.0; 75:25) (Breda et al. 1993). The equipment consisted of Shimadzu ultraviolet (UV)–vis detector and reversed phase C-18 column, Lichro Cart-RP8 (250×4.6 mm, 5 μ). The mobile phase was delivered at a flow rate of 1.0 ml/min, the injection volume was 20 μl, the effluent was monitored at UV detection at 247 nm, and the retention time for exe was 5.0 min.

2.8 Drug content and percentage drug entrapment

The drug content in the NPs was determined by dissolving 10 mg of lyophilized NPs in 10 ml of acetonitrile for analysis by HPLC after filtration through 0.22 μ and appropriate dilution with mobile phase. Drug loading was calculated as follows:

$$\mathrm{DL}(\%) = A \Big/ B \times 100$$

where, A is the drug content in the NPs and B is the weight of NPs. It was confirmed from preformulation studies that cPCL, Poloxamer 188, and sucrose did not interfere in the analysis of exe. PDE was estimated by calculating amount of drug entrapped in NPs with respect to total drug added during preparation of formulation and free drug which was estimated from the supernatant after centrifugation at 50,000×g.

The PDE was calculated according to following formula:

$$\mathrm{PDE} = \left(\mathrm{TD}-\mathrm{FD} \Big/ \mathrm{TD}\right) \times 100$$

where, TD is total amount of drug added and FD is amount of drug in supernatant.

2.9 Particle size and zeta potential

The size analysis and polydispersity index of the NPs were determined using a Malvern Zetasizer Nano ZS (Malvern Instrument, Worcestershire, UK). Each sample was diluted ten times with filtered distilled water to avoid multiscattering phenomena and placed in disposable sizing cuvette. Polydispersity index was noted to determine the narrowness of the PS distribution. The size analysis was performed in triplicate, and the results were expressed as mean size±SD.

Zeta potential distribution was also measured using a Zetasizer (Nano ZS, Malvern instrument, Worcestershire, UK). Each sample was suitably diluted ten times with filtered distilled water and placed in a disposable zeta cell. Zeta limits ranged from −200 to +200 mV. The electrophoretic mobility (μm/sec) was converted to zeta potential by in-built software using Helmholtz-Smoluchowski equation. Average of 3 measurements of each sample was used to derive average zeta potential.

2.10 Experimental design

A three-factor, three-level Box–Behnken statistical design was employed to optimize the process and formulation parameters in preparation of exe-loaded cPCL NPs and evaluate main effects, interaction effects, and quadratic effects of the process parameters on the PDE and PS. The independent variables selected were drug/polymer ratio (X_1), amount of cPCL (X_2), and volume of organic phase (X_3). A design matrix comprising 13 experimental runs was constructed. The design was used to explore quadratic response surfaces and constructing second-order polynomial models and contour plots to predict responses with Design Expert (Version 8.0.3, Stat-Ease Inc., Minneapolis, MN).

2.11 Contour plots

Contour plots are diagrammatic representation of the values of the response. They are helpful in explaining the relationship between independent and dependent variables. The reduced models were used to plot two-dimensional contour plots. Two contour plots for PDE and PS were established between X_2 and X_3 at fixed levels (−1, 0, and 1) of X_1.

2.12 Response surface plots

To understand the main and the interaction effects of two variables, response surface plots were used as a function of two factors at a time, maintaining the third factor at fixed level (Mak et al. 1995). These plots were obtained by calculating the values obtained by one factor where the second varied (from −1 to 1 for instance) with constraint of a given Y value.

2.13 Check point analysis

A check point analysis was performed to confirm the utility of the established contour plots and reduced polynomial equation in the preparation of NPs. Values of independent variables (X_2 and X_3) were taken from three check points on contour plots plotted at fixed levels of −1, 0, and 1 of X_1, and the values of PDE (Y_1) and PS (Y_2) were calculated by substituting the values in the reduced polynomial equation. Exe-loaded NPs were prepared experimentally by taking the amounts of the independent variables (X_1 and X_2). Each batch was prepared three times and mean values were determined. Difference in the predicted and mean values of experimentally obtained PDE and PS was compared by using student's t test.

2.14 Normalized error determination

The quantitative relationship established by BBD was confirmed by evaluating experimentally prepared exe-loaded NPs. PDE and PS predicted from the BBD were compared with those generated from prepared batches of check point analysis using normalized error (NE). The equation of NE (Eq. 1) is expressed as follows:

$$NE = \left[\Sigma\left\{(\text{Pre} - \text{Obs})\Big/\text{Obs}\right\}^2\right]^{1/2} \quad (1)$$

where, Pre and Obs represent predicted and observed response, respectively.

2.15 Desirability criteria

For simultaneous optimization of PDE and PS, desirability function (multiresponse optimization technique) was applied and total desirability was calculated using Design Expert software. The desirability lies between 0 and 1, and it represents the closeness of a response to its ideal value. The total desirability is defined as a geometric mean of the individual desirability for PDE and PS (Derringer and Suich 1980).

$$D = \left(d_{\text{PDE}} X\, d_{\text{PS}}\right)^{1/2} \quad (2)$$

where, D is the total desirability, d_{PDE} and d_{PS} are individual desirability for PDE and PS. If both the quality characteristics reach their ideal values, the individual desirability is 1 for both. Consequently, the total desirability is also 1. Our criteria included highest possible PDE and PS of less than 200 nm.

2.16 In vitro drug release studies

In vitro release of exe from cPCL NPs was evaluated by the dialysis bag diffusion technique in phosphate buffered saline (PBS; pH 7.4) (Yang et al. 1999). The aqueous nanoparticulate dispersion equivalent to 2 mg of exe was placed in a dialysis bag (cut-off 12,000 Da; Himedia, Mumbai, India), which was previously soaked overnight in water, cleaned next morning and sealed at both ends. The dialysis bag was immersed in the receptor compartment containing 50 ml of PBS (pH 7.4), which was stirred at 100 rpm and maintained at 37±2 °C. The receptor compartment was covered to prevent the evaporation of release medium. Samples (2 ml) were withdrawn at regular time intervals; the same volume was replaced by fresh release medium and measured for amount of exe released using previously described HPLC method (Breda et al. 1993; Mendes et al. 2007). All the experiments were performed in triplicate, and the average values were taken. Exe suspension prepared in PBS (pH 7.4) was used as a control. The kinetic analysis of the release data was done using Korsmeyer and Peppas equation or the Power law equation (Peppas 1985):

$$M_t \Big/ M_\infty = \text{kt}^n \quad (3)$$

Where, M_t/M_∞ is the fractional amount of drug released, k is the release constant, n is the release exponent, and t is the time of release.

2.17 Transmission electron microscope studies

A sample of NPs (0.5 mg/ml) was suspended in water and bath sonicated for 30 s; 2 μl of this suspension was placed over a Formvar-coated copper transmission electron microscopy (TEM) grid (150 meshes) and negatively stained with 2 μl uranyl acetate (1 %) for 10 min, allowed to dry, and the images were visualized at 80 kV under TEM (FEI Tecnai G2 Spirit Twin, Czech Republic) and captured using Gatan Digital Micrograph software.

2.18 Differential scanning calorimetric studies

All the samples were dried in desiccators for 24 h before thermal analysis. Differential scanning calorimetry (DSC) studies on pure exe, cPCL, physical mixtures of drug and cPCL and drug-loaded NPs were performed in order to characterize the physical state of drug in the NPs. Thermograms were obtained using DSC model 2910 (TA Instruments, New Castle, DE). Dry nitrogen gas was used as the purge gas

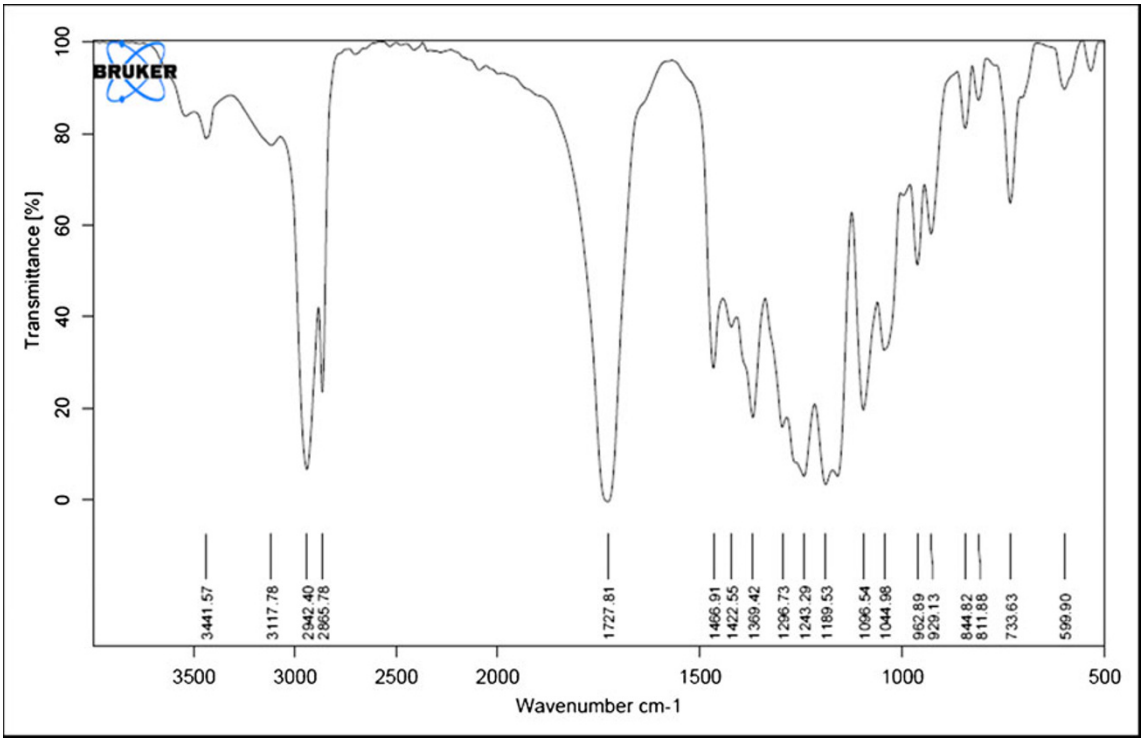

Fig. 1 FTIR spectra of cPCL

through the DSC cell at a flow rate of 40 ml/min. Samples (4–8 mg) were sealed in standard aluminum pans with lids and heated at a rate of 10 °C/min from 20 to 300 °C. Data were analyzed using TA Universal Analysis 2000 software (TA Instruments, New Castle, DE).

3 Results and discussion

Successful polymerization of caprolactone to cPCL was confirmed by FTIR spectra of polymer (Fig. 1). The peak at 1,727.81 cm^{-1} corresponding to carboxylic group and 3,441 cm^{-1} for OH stretching of COOH group confirmed the conversion of caprolactone to cPCL (Zhang et al. 1994). Molecular weight of cPCL was found to be 17,487±276 Da using GPC (Fig. 2) which was found to be close to theoretically predicted molecular weight (17,814 Da). Thirteen batches of exe-loaded cPCL NPs were prepared as per BBD changing three independent variables, drug/polymer ratio (X_1), amount of polymer (X_2), and volume of organic phase (X_3). Coded values and actual values of the three independent variables, drug/polymer ratio (X_1), surfactant concentration (X_2), and volume of organic phase (X_3) are represented in Table 1. Batches prepared using BBD were evaluated for PDE and PS as the dependent variables and recorded in Table 2. The obtained PDE and PS were subjected to multiple regression to yield second-order polynomial equations (Eqs. 4 and 5, for PDE and PS, respectively). Linear coefficients (b_1, b_2, and b_3 of X_1, X_2, and X_3, respectively) represent extent of effect by changing individual variable. Positive or negative sign in equation against different coefficients indicate increase or decrease in individual-dependent response. The value of coefficients against interactions terms (X_1X_2, X_1X_3, and X_2X_3) shows how the PDE and PS changes when two variables were simultaneously changed. The values of all the 13 batches showed wide variation of 23.94±1.25 to 82.68±1.31 % and 115.03±3.60 to 350.03±7.21 nm for PDE and PS, respectively as shown in Table 2. This variation is reflected by the wide range of coefficients of the terms representing the individual and combined variables. The significance of each coefficient of Eqs. 4 and 5 was determined by student's t test and p value, which are listed in Tables 3 and 4, respectively. The larger the magnitude of the t value and the smaller the p value, the more significant is the corresponding coefficient (Akhnazarova and Kafarov 1982; Adinarayana and Ellaiah 2002). Small values of the coefficients of the terms X_1, X_1X_2, X_1X_3, and X_1^2 in Eq. 4 and X_1, X_1X_2, X_1X_3, X_2^2, and X_3^2 in Eq. 5 implied that all these terms were least contributing in the preparation of exe-loaded cPCL NPs. These small values of coefficients had $p>0.05$. Hence, these terms were neglected from the full model considering nonsignificance and reduced polynomial equations (Eqs. 6 and 7, for PDE and PS, respectively) were obtained following regression analysis of PDE and PS. From reduced model, it was evident that drug/polymer ratio did not affect any of the dependent variables significantly ($p>0.05$). The interaction effects of X_1X_2 and X_1X_3 was also found to be

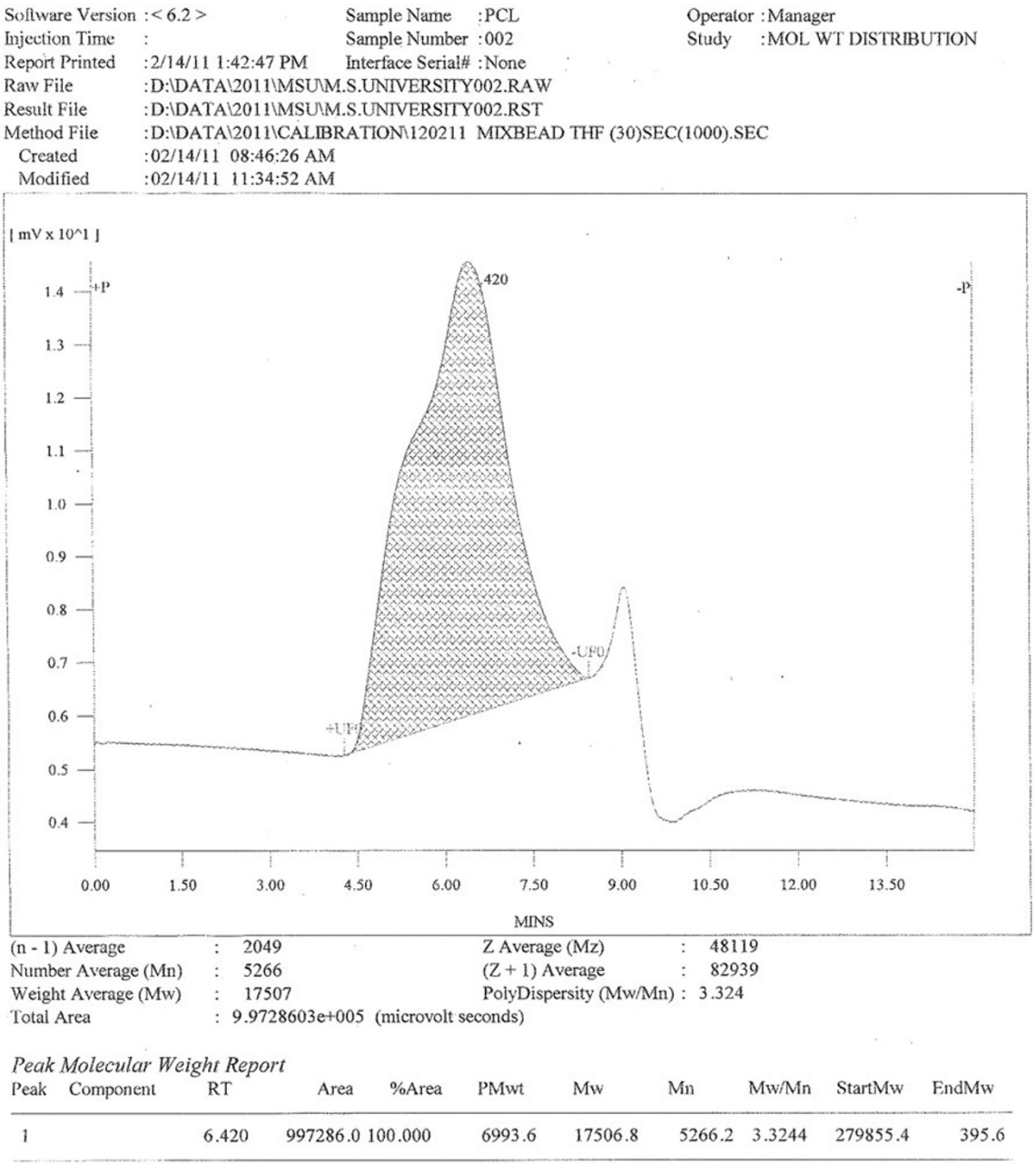

Fig. 2 Gel permeation chromatogram of cPCL showing molecular weight of synthesized polymer as 17,507 Da

Table 1 Coded values of the formulation parameters of exemestane-loaded cPCL NPs

Coded values	Actual values		
	X_1	X_2 (mg)	X_3 (ml)
−1	1:15	50	6
0	1:20	100	8
1	1:25	150	10

X_1 drug/polymer ratio, X_2 amount of polymer (in milligrams), X_3 volume of organic phase (in milliliters)

nonsignificant ($p>0.05$) for both PDE and PS. For PDE, the quadratic effect of drug/polymer ratio, while for PS, the quadratic effect of amount of polymer and volume of organic phase were insignificant (Tables 3 and 4). PS distribution of NPs and HPLC chromatogram of drug is shown in Figs. S-1 and S-2, respectively, in the Electronic supplementary material.

$$Y_1 = 82.68 + 3.26X_1 - 6.84X_2 + 13.25X_3 + 2.51X_1X_2 + 6.63X_1X_3 + 7.98X_2X_3 - 4.27X_1^2 - 10.98X_2^2 - 15.07X_3^2 \quad (4)$$

Table 2 Box–Behnken experimental design with measured responses for exemestane-loaded cPCL NPs

Sr. No.	X_1	X_2	X_3	Y_1 (PDE, mean±SD)	Y_2 (PS, mean±SD)
1	0	−1	−1	56.32±1.738	224.10±7.213
2	0	−1	1	73.36±2.081	115.03±3.595
3	0	1	−1	23.94±1.254	263.67±4.549
4	0	1	1	72.89±1.437	256.27±5.387
5	−1	0	−1	57.93±1.728	284.77±4.879
6	−1	0	1	64.68±1.921	185.00±4.424
7	1	0	−1	48.71±0.713	302.63±2.875
8	1	0	1	82.00±1.101	212.40±3.050
9	−1	−1	0	70.91±1.788	185.93±3.502
10	−1	1	0	54.94±1.806	340.43±8.334
11	1	−1	0	74.89±2.644	235.80±6.777
12	1	1	0	68.95±3.235	350.03±7.214
13	0	0	0	82.67±1.310	207.40±2.035

$$Y_2 = 207.41 + 13.08X_1 + 56.19X_2 - 38.32X_3 - 10.06X_1X_2 + 2.38X_1X_3 + 25.42X_2X_3 + 51.04X_1^2 + 19.61X_2^2 - 12.25X_3^2 \quad (5)$$

$$Y_1 = 77.79 - 6.84X_2 + 13.25X_3 + 7.98X_2X_3 - 9.14X_2^2 - 13.23X_3^2 \quad (6)$$

$$Y_2 = 213.29 + 56.19X_2 - 38.32X_3 + 25.42X_2X_3 + 48.83X_1^2 \quad (7)$$

The results of ANOVA of the second-order polynomial equation of PDE and PS are given in Tables 5 and 6, respectively. Since the calculated F value (1.3911) is less than the tabulated F value (9.0135; α=0.05, V_1=5, and V_2=3) for PDE, and calculated F value (2.2086) is less than the tabulated F value (9.1172; α=0.05, V_1=4, and V_2=3) (Bolton and Bon 1997) for PS, it was concluded that the neglected terms did not significantly contribute in the prediction of PDE and PS. Thus, the results of ANOVA of full and reduced model justified the omission of nonsignificant terms of Eqs. 4 and 5. When the coefficients of the three independent variables in Eqs. 6 and 7 were compared, the values for the variables X_3 (13.25) for PDE and X_2 (56.19) for PS were found to be maximum and hence these variables were considered to be major contributing variables affecting the PDE and PS of the NPs. The Fisher F test with a very low probability value ($P_{model}>F$=0.000001) demonstrated a very high significance for the derived regression model.

The goodness of fit of the model was checked by the determination coefficient (R^2). In this case, the values of the determination coefficients (R^2=0.9681 and 0.9634 for

Table 3 Model coefficients estimated by multiple regression analysis for PDE of exemestane-loaded cPCL NPs

Factor	Coefficients	t stat	p value
Intercept	82.67	13.5711	0.0009*
X_1	3.2596	1.5135	0.2274
X_2	−6.8440	−3.1777	0.0482*
X_3	13.2531	6.1536	0.0086*
X_1X_2	2.5067	0.8230	0.4708
X_1X_3	6.6334	2.1779	0.1176
X_2X_3	7.9769	2.6190	0.0491*
X_1^2	−4.2709	−1.0600	0.3669
X_2^2	−10.9755	−2.7240	0.0423*
X_3^2	−15.0662	−3.7392	0.0334*

*p<0.05, significance level

Table 4 Model coefficients estimated by multiple regression analysis for PS of exemestane-loaded cPCL NPs

Factor	Coefficients	t stat	p value
Intercept	207.4	8.7941	0.0031*
X_1	13.0775	1.5684	0.2148
X_2	56.1863	6.7384	0.0067*
X_3	−38.3225	−4.5960	0.0194*
X_1X_2	−10.0588	−0.8530	0.4563
X_1X_3	2.3788	0.2017	0.8530
X_2X_3	25.4188	2.1556	0.0301*
X_1^2	51.0381	3.2718	0.0467*
X_2^2	19.6131	1.2573	0.2976
X_3^2	−12.2444	−0.7849	0.4898

*p<0.05, significance level

Table 5 Analysis of variance of full and reduced models for PDE of exemestane-loaded cPCL NPs

		df	SS	MS	*F*	*R*	R^2	Adjusted R^2
Regression	FM	9	50,793.04	5,643.672	10.1466	0.9839	0.9681	0.8727
	RM	4	46,924.29	11,731.07	16.9481	0.9457	0.8944	0.8416
Residual	FM	3	1,668.632	556.2107				
	RM	8	5,537.387	692.1734				

SSE2−SSE1=5,537.387−1,668.632=3,868.755. No. of parameters omitted=5. MS of error (full model)=556.2107. *F* calculated=(SSE2−SSE1/No. of parameters omitted)/MS of error (FM)=(3,868.755/5)/556.2107=1.3911

PDE and PS, respectively) indicated that over 96 % of the total variations were explained by the model. After reducing the equation, the values of the determination coefficients (R^2=0.8944 and 0.8558 for PDE and PS, respectively) indicated that over 85 % of the total variations were explained by the model. High R^2 values of full model as compared with reduced model are possibly due to the number of factors included. The more the number of factors, the more is the R^2 value, even if the factors are not significant (Montgomery 2004). The values of adjusted determination coefficients (adj R^2= 0.8727 and 0.8538 for PDE and PS, respectively) were also very high (>85 %) indicating high significance of the model. Moreover, the high values of correlation coefficients (R=0.9839 and 0.9815 for PDE and PS, respectively) signify an excellent correlation between the independent variables (Box et al. 1978). All the above considerations indicate an excellent adequacy of the derived regression model (Akhnazarova and Kafarov 1982; Adinarayana and Ellaiah 2002; Box et al. 1978; Yee and Blanch 1993).

3.1 Contour plots

Values of X_1, X_2, and X_3 were computed for PDE and PS, and contour plots were established between X_1 vs. X_2, X_1 vs. X_3, and X_2 vs. X_3 at fixed level (+1) of third variable as shown in Figs. 3 and 4 for each PDE and PS, respectively. Contour plots showed that PDE was greatly dependent on drug:polymer ratio and amount of polymer (Fig. 3a). PDE was found to be maximum at high level of X_1 and mid- to high level of X_2. PDE was found to be more than 60 % in the whole range of −1 to +1 for both X_1 and X_2 at +1 level of X_3. Contour plot of drug/polymer ratio vs. volume of organic phase showed maximum PDE of more than 70 % at 0 to +1 value of X_1 and +0.1 to +1.0 value of X_3 at +1 level of X_2 (Fig. 3b). PDE remained to be less than 80 % in the whole range (−1 to +1) of both variables. Contour plot of amount of polymer vs. volume of organic phase at +1 level of drug/polymer ratio indicated PDE of more than 80 % when X_2 varied from −0.5 to 0.9 level and X_3 from 0 to +1.0 level (Fig. 3c). Lowest PS of about 175 nm was observed at −0.5 to 0 level of drug/polymer ratio, −0.8 to −1.0 level of amount of polymer at +1 level of volume of organic phase (Fig. 4a). When drug/polymer ratio was varied with volume of organic phase, PS was less than 275 nm at −0.5 to 0.5 level of X_1 and 0.5 to 1.0 level of X_3 at +1 level of X_2 (Fig. 4b). From Fig. 4c, it is evident that at highest level of drug/polymer ratio (+1.0), PS increased as the amount of polymer increased (−1.0 to +1.0), and volume of organic phase decreased (+1.0 to −1.0), PS increases. It was concluded from the contours that high drug/polymer ratio, low amount of polymer, and highest volume of organic phase were required for preparation of exe NPs with highest PDE and lowest PS.

3.2 Response surface plots

Response surface plots are very important tools in learning both the main and interaction effects of the independent variables. Response surface plots were plotted between X_1 vs. X_2, X_1 vs. X_3 and X_2 vs. X_3 at fixed level (+1) of third variable as

Table 6 Analysis of variance of full and reduced models for PS of exemestane-loaded cPCL NPs

		df	SS	MS	*F*	*R*	R^2	Adjusted R^2
Regression	FM	9	2,935.152	326.128	8.7886	0.9815	0.9634	0.8538
	RM	5	2,607.316	521.4632	8.3118	0.9251	0.8558	0.7528
Residual	FM	3	111.3241	37.1080				
	RM	7	439.1605	62.7372				

SSE2−SSE1=439.1605−111.3241=327.8364. No. of parameters omitted=4. MS of error (full model)=37.1080. *F* calculated=(SSE2−SSE1/No. of parameters omitted)/MS of error (FM)=(327.8364/4)/37.1080=2.2086

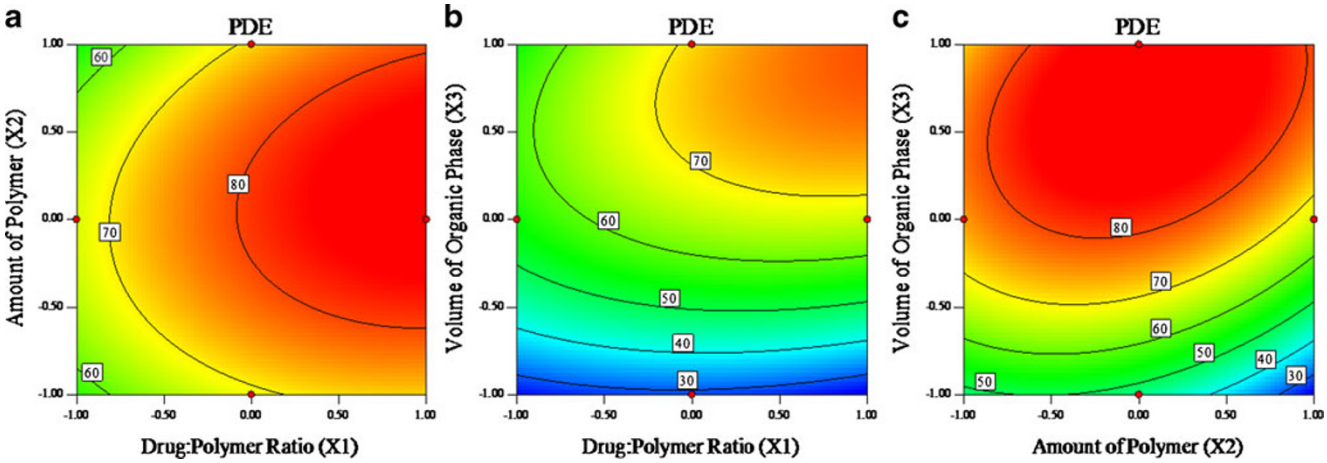

Fig. 3 Contour plots showing effect of **a** X_1 vs. X_2 (at +1 level of X_3), **b** X_1 vs. X_3 (at +1 level of X_2), and **c** X_2 vs. X_3 (at +1 level of X_1) on PDE of exe-loaded cPCL NPs

shown in Figs. 5 and 6 for PDE and PS respectively. PDE was found to first increase with increase in amount of polymer, and further increase caused decrease in PDE. PDE was maximum at highest level of drug/polymer ratio and mid-level of amount of polymer (Fig. 5a). The volume of organic phase had more significant effect on the outcome of PDE. PDE decreased sharply with decrease in volume of organic phase. However, PDE was not found to be much influenced by changing the drug/polymer ratio (Fig. 5b). PDE was found to decrease with increase in amount of polymer. Decrease in volume of organic phase and increase in amount of polymer resulted in overall decrease in PDE (Fig. 5c).

Response surface plot of drug/polymer ratio vs. amount of polymer showed nonlinear behavior. With decrease in drug/polymer ratio, no significant change in PS was observed. Simultaneous increase in both drug/polymer ratio as well as polymer concentration showed increased PS. Increase in PS was more influenced by change in amount of polymer than drug/polymer ratio (Fig. 6a). Response surface plot between drug/polymer ratio and volume of organic phase showed no significant change in PS (Fig. 6b). Plot between amount of polymer and volume of organic phase showed increase in PS when amount of polymer increased and volume of organic phase decreased at the same time (Fig. 6c).

3.3 Desirability criteria

From the results, the optimum levels of independent variables were screened out by regression analysis. Since PDE and PS were taken into consideration simultaneously, the results were unable to attend both the dependent variables at a time. The batch with smallest PS of less than 175 nm exhibited only about 69-71 % PDE (at X_1=−0.5 to 0, X_2=−0.8 to −1.0, and X_3=+1.0) while that with highest PDE of more than 80 % had PS of 210 to 300 nm (at X_1=+1, X_2=−0.5 to 0.9, and

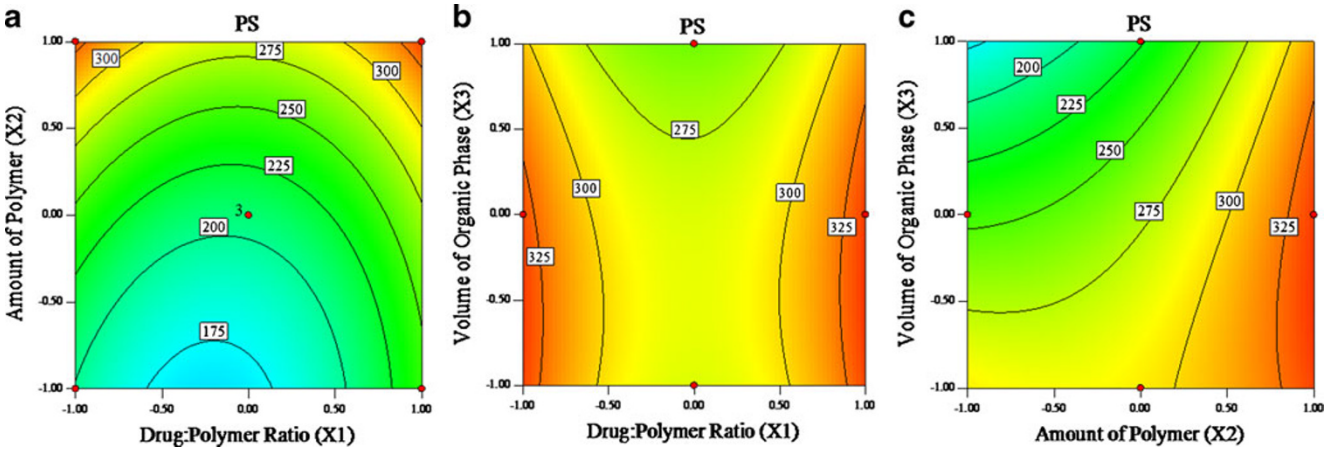

Fig. 4 Contour plots showing effect of **a** X_1 vs. X_2 (at +1 level of X_3), **b** X_1 vs. X_3 (at +1 level of X_2), and **c** X_2 vs. X_3 (at +1 level of X_1) on PS of exe-loaded cPCL NPs

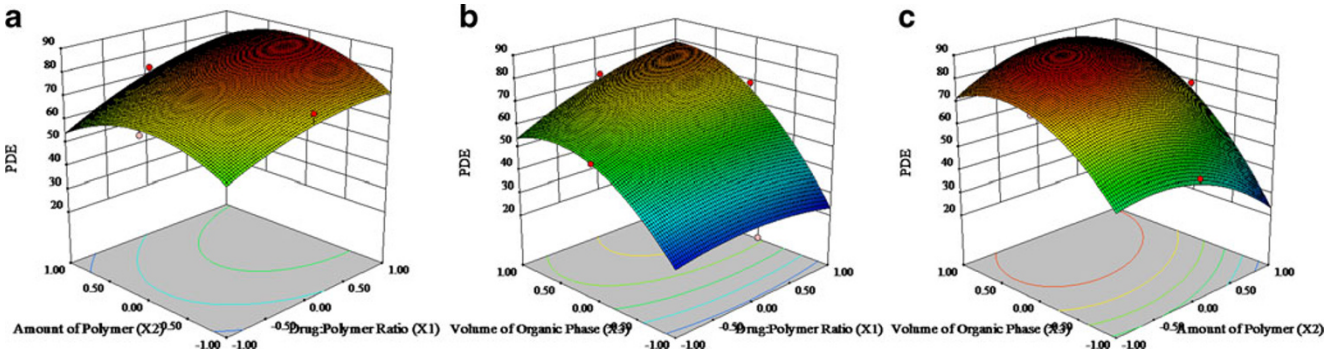

Fig. 5 Response surface plot showing effect of **a** X_1 vs. X_2 (at +1 level of X_3), **b** X_1 vs. X_3 (at +1 level of X_2) and **c** X_2 vs. X_3 (at +1 level of X_1) on PDE of exe-loaded cPCL NPs

X_3=0 to +1.0) (Figs. 3 and 4). Hence, desirability criteria were used to find out optimized formulation parameters. The desirability criteria were obtained using Design Expert software (version 8.0.3). Our criteria included maximum PDE and PS not more than 200 nm. The optimum formulation offered by the Design Expert 8.0.3 software based on desirability was found at 0.43, −0.68, and 0.27 level of X_1, X_2, and X_3 respectively. The calculated desirability factor for offered formulations was 1, which indicated suitability of the designed factorial model. The results of dependent variables from the software were found to yield 83.96 % PDE and 180.51 nm PS at these levels.

3.4 Checkpoint analysis and NE

Three batches were prepared for check point analysis and evaluated for PDE and PS as shown in Table 7. Results indicated that the measured response was more accurately predicted by regression analysis which was proved by lower NE value of regression analysis (0.04167 for PDE and 0.02591 for PS). Data analysis using student's *t* test revealed that there was no statistically significant difference ($p<0.05$) between experimentally obtained values and predicted values by regression analysis and hence, it confirms the utility of the established contour plots and reduced polynomial equation in the preparation of NPs.

3.5 Zeta potential

Zeta potential gives information to predict the storage stability of colloidal dispersions (Thode et al. 2000). High negative values of the zeta potential indicate that the electrostatic repulsion between particles will prevent their aggregation and thereby stabilize the nanoparticulate dispersion (Feng and Huang 2001; Joshi et al. 2010). The zeta potential values ranged between −19.6 and −34.0 mV for all 13 formulations. The surfactant concentration affected the charge on the particle. It was seen that as the surfactant concentration was increased from 0.25 to 0.75 %, there was a decrease in the zeta potential value. This is possibly because with increase in concentration of non-ionic surfactant, total charge on the particle decreases due to increased amount of surfactant coating which also resulted in increased PS (Redhead et al. 2001). However, change in polymer concentration had no effect on zeta potential values. The optimized batch of exe-loaded cPCL NPs was found to have zeta potential of −33.8±2.1 mV. Zeta potential values in the −15 to −30 mV are common for well-

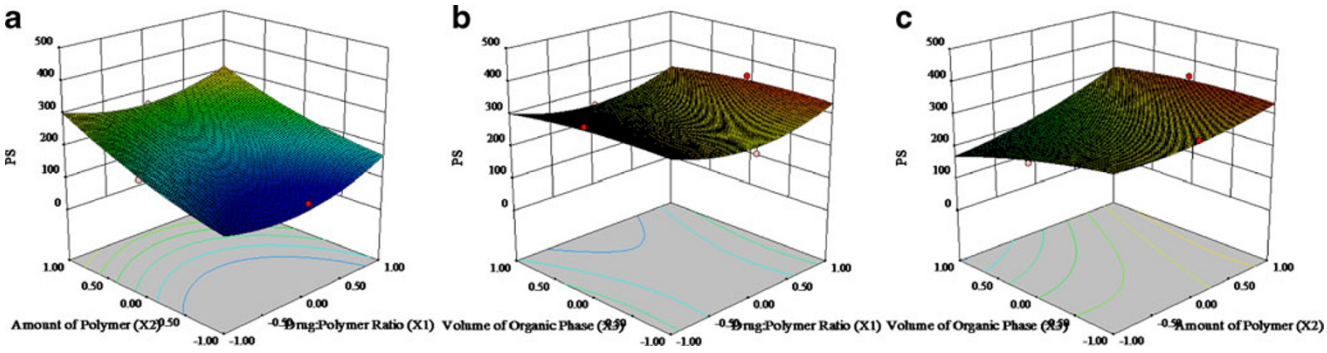

Fig. 6 Response surface plot showing effect of **a** X_1 vs. X_2 (at +1 level of X_3), **b** X_1 vs. X_3 (at +1 level of X_2), and **c** X_2 vs. X_3 (at +1 level of X_1) on PS of exe-loaded cPCL NPs

Table 7 Check point analysis, *t* test analysis, and normalized error determination

Batch No.	X_1	X_2	X_3	PDE		PS	
				Observed (average)	Predicted	Observed (average)	Predicted
1	−1 (1:15)	−0.3 (85 mg)	0.5 (9 ml)	84.14	85.93	225.6	222.29
2	0 (1:20)	0.2 (110 mg)	−0.8 (6.4 ml)	58.63	57.08	256.4	251.12
3	1 (1:25)	−0.7 (65 mg)	0.8 (9.6 ml)	65.72	64.13	176.9	177.9
$t_{calculated}$				0.7267		0.3057	
$t_{tabulated}$				2.9199		2.9199	
Normalized error				0.04167		0.02591	

stabilized NPs (Musumeci et al. 2006). Hence, it was concluded that the NPs would remain physically stable.

3.6 Lyophilization and optimization of cryoprotectants

Cryoprotectants are important in retaining PS upon reconstitution. Freeze drying causes increase in PS of NPs after lyophilization due to aggregation of particles during the process (Abdelwahed et al. 2006). If these aggregates are not separated during re-dispersion, it may cause instability to the system. In this study, different cryoprotectants (trehalose, sucrose, and mannitol) were used in different ratios (1:1, 1:2, 1:3, and 1:4) and PS was recorded as shown in Table 8. Initial PS of NPs was found to be 180.5 nm. The ratio of PS (after lyophilization (S_f) and before lyophilization (S_i)) was found to be lowest (1.22) for sucrose in 1:2 ratio and considered optimum. Trehalose also showed less increase in PS after re-dispersion (S_f/S_i ratio of 1.39). Trehalose and sucrose at 1:1, 1:2, and 1:3 ratio showed less S_f/S_i ratio indicating good re-dispersibility with PDI less than 0.2. PDI is a measure of dispersion homogeneity and usually ranges from 0 to 1. Values close to 0 indicate a homogeneous dispersion while those greater than 0.3 indicate high heterogeneity (Ahlin et al. 2002).

Table 8 Effect of cryoprotectants and their concentration on PS of lyophilized NPs after re-dispersion in distilled water

Cryoprotectant	Ratio	Final average PS in nm (S_f)	S_f/S_i
Trehalose	1:1	254.0	1.41[a]
	1:2	250.6	1.39[a]
	1:3	288.4	1.60[a]
	1:4	315.9	1.75
Sucrose	1:1	232.4	1.29[a]
	1:2	220.7	1.22[a]
	1:3	273.5	1.52[a]
	1:4	298.1	1.65
Mannitol	1:1	275.9	1.53
	1:2	290.2	1.61
	1:3	318.0	1.76
	1:4	348.5	1.93

[a] Good re-dispersibility

3.7 Transmission electron microscopy

TEM image of exe-loaded cPCL NPs is shown in Fig. 7. The image reveals that the particles were discrete, round and uniform in shape with diameters in the range of 80–100 nm. The higher hydrodynamic diameter of NPs achieved by DLS analysis as compared with the size obtained by TEM analysis may be contributed by the hydration of the surface associated Poloxamer (Das and Sahoo 2012; Misra and Sahoo 2010).

3.8 Differential scanning calorimetry

DSC is a helpful technique for investigation of thermal properties of a formulation, providing information about

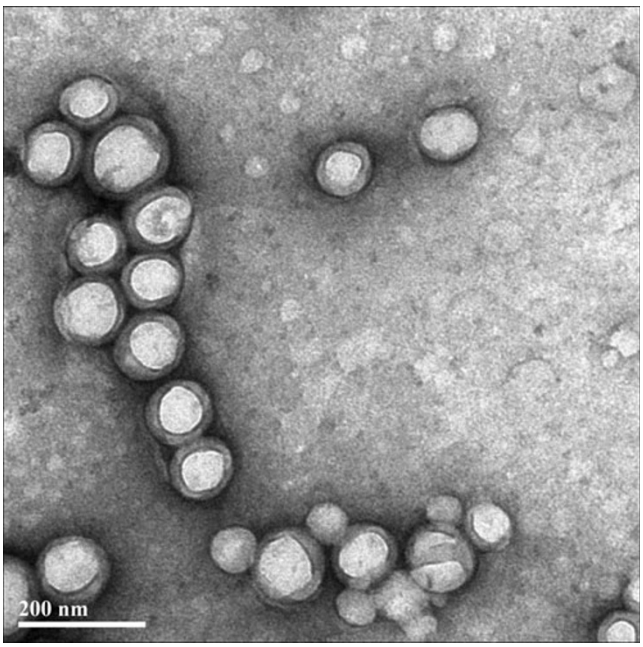

Fig. 7 TEM image of exe-loaded cPCL NPs

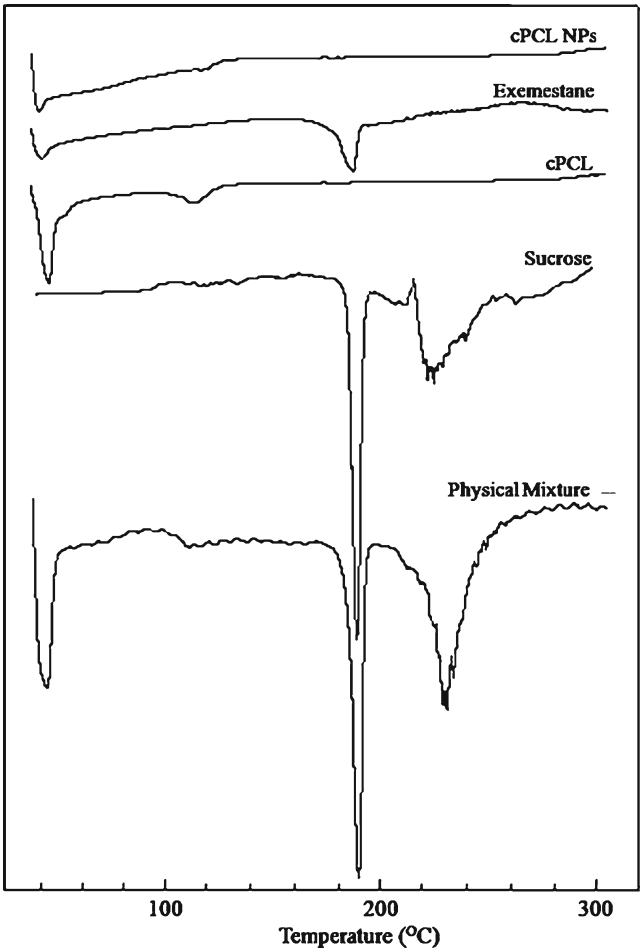

Fig. 8 DSC thermogram of exe-loaded cPCL NPs (**a**), exe (**b**), cPCL (**c**), sucrose (**d**), and physical mixture (**e**)

physicochemical state of drug in the delivery system. DSC thermograms of pure exe, cPCL polymer, sucrose, physical mixture, and exe-loaded cPCL NPs are shown in Fig. 8. Pure exe showed an endothermic melting peak at 182.56 °C indicating its crystalline nature. cPCL showed endothermic peak at 47.65 °C, which was lower than the reported melting point of PCL (60 °C) It has been reported that modifications in polymer or polymer structure will change its melting point (Orozco-Castellanos et al. 2011). Thus, the lowering of melting point of PCL in cPCL can be taken as an indication of its carboxylation, which was also confirmed by FTIR and GPC. There was no peak of exe in the thermogram of NPs indicating that exe may be existing as a molecular dispersion or in an amorphous phase in the polymer matrix (Kashi et al. 2012). It is reported that no detectable endotherm will be observed if the drug is present in a molecular dispersion or solid solution state in the polymeric NPs (Dubernet 1995). However, as the drug is crystalline, total disappearance of its peak in the thermogram of the NPs indicate towards its existence as a molecular dispersion rather than amorphous form.

3.9 In vitro drug release studies

In vitro release of exe from plain drug suspension and NPs is shown in Fig. 9. Within 6 h, 99.08±0.88 % drug release occurred from plain drug suspension, whereas only 26.36± 0.67 % drug release occurred from NPs, reaching 44.89± 1.30 % after 120 h and 70.67±1.76 % after 240 h, indicating sustained release. Thus, it was clear that incorporation of exe in cPCL NPs could significantly sustain its release. The drug release from NPs followed biphasic release model with an initial burst release for about 6 h followed by sustained release for more than 240 h. The burst release may be attributed to the drug molecules associated near particle surface (Seju et al. 2011). Also, particles of nanosize range lead to a shorter average diffusion path for the matrix entrapped drug molecules, thereby causing faster diffusion (Shah et al. 2009; Mainardes and Evangelista 2005). After initial burst release, the release rate decreased, reflecting the release of drug entrapped in the polymer matrix. The release rate in the second phase was assumed to be controlled by

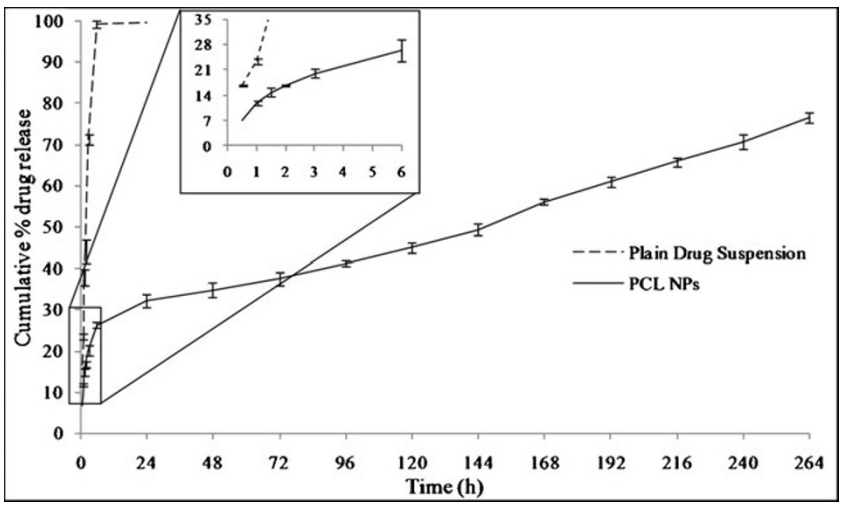

Fig. 9 Drug release profile of exe from plain drug suspension and cPCL NPs across semipermeable membrane using the dialysis bag diffusion technique in phosphate-buffered saline (pH 7.4). The values represent mean±SD of three batches

diffusion rate of drug across the polymer matrix (Corrigan and Li 2009). The data obtained from in vitro drug release studies was fitted to Korsmeyer–Peppas model. The release constant (k) of the plot of log M_t/M_∞ versus log t for NPs was found to be 0.9519 with value of release exponent (n) as 0.3057. The n value is the release exponent which characterizes the transport mechanism and if its value is less than 0.5, it indicates Fickian release (Peppas 1985; Yadav and Sawant 2010). Hence, it was concluded that the release of exe from NPs was by Fickian diffusion.

4 Conclusions

Caprolactone was successfully polymerized in presence of succinic acid to PCL by ring opening polymerization. The present study demonstrated the use of Box–Behnken design as data analysis approach to understand the effect of various formulation variables in the prediction of PDE and PS of exe-loaded cPCL NPs. No significant difference between predicted and observed responses was observed in check point analysis with very less NE. The optimized cPCL NPs of exe had high entrapment and small PS. DSC studies indicated absence of any interaction of exe with cPCL. These NPs exhibited sustained release and followed Fickian diffusion based release kinetics. This sustained release delivery system of exe would reduce the side effects associated with the conventional cancer therapy by reducing dosing frequency and systemic side effects. Thus, our results prove that desirable goals can be achieved by systematic statistical approach in shortest possible time with reduced number of experiments.

Acknowledgments The authors are grateful to All India Council of Technical Education, New Delhi, India for providing National Doctoral Fellowship to Abhinesh Kumar. We also acknowledge Sun Pharma Advanced Research Centre, Vadodara, India for gift sample of exe, Abitec Corporation, Janesville, WI for Capric/caprylic triglyceride (Capmul MCM, C8) and BASF, Ludwigshafen, Germany for Poloxamer 188.

Declaration of interests The author(s) declare that they have no competing interests.

References

Abdelwahed W, Degobert G, Stainmesse S, Fessi H (2006) Freeze-drying of nanoparticles: formulation, process and storage considerations. Adv Drug Deliv Rev 58(15):1688–1713

Aberturas MR, Perez H, de la Ossa D, Gil ME, Ligresti A, De Petrocellis L, Torres AI, Di Marzo V, Molpeceres J (2011) Anandamide-loaded nanoparticles: preparation and characterization. J Microencapsul 28(3):200–210

Adinarayana K, Ellaiah P (2002) Response surface optimization of the critical medium components for the production of alkaline protease by a newly isolated Bacillus sp. J Pharm Pharm Sci 5(3):272–278

Ahlin P, Kristl J, Kristl A, Vrečer F (2002) Investigation of polymeric nanoparticles as carriers of enalaprilat for oral administration. Int J Pharm 239(1–2):113–120

Akhnazarova S, Kafarov V (1982) Experiment optimization in chemistry and chemical engineering. MIR Publications, Moscow

Bae S, Shoda M (2005) Statistical optimization of culture conditions for bacterial cellulose production using Box–Behnken design. Biotechnol Bioeng 90(1):20–28

Barichello JM, Morishita M, Takayama K, Nagai T (1999) Encapsulation of hydrophilic and lipophilic drugs in PLGA nanoparticles by the nanoprecipitation method. Drug Dev Ind Pharm 25(4):471–476

Behan N, Birkinshaw C, Clarke N (2001) Poly *n*-butyl cyanoacrylate nanoparticles: a mechanistic study of polymerisation and particle formation. Biomaterials 22(11):1335–1344

Bolton S, Bon C (1997) Pharmaceutical statistics: practical and clinical applications, 3rd edn. Marcel Dekker, New York

Box GEP, Hunter WG, Hunter WS (1978) Statistics for experimenters: an introduction to design, data analysis, and model building. Wiley, New York

Breda M, Pianezzola E, Benedetti MS (1993) Determination of exemestane, a new aromatase inhibitor, in plasma by high-performance liquid chromatography with ultraviolet detection. J Chromato 620(2):225–231

Chacon M, Molpeceres J, Berges L, Guzman M, Aberturas MR (1999) Stability and freeze-drying of cyclosporine loaded poly(D,L lactide-glycolide) carriers. Eur J Pharm Sci 8(2):99–107

Clemett D, Lamb HM (2000) Exemestane: a review of its use in postmenopausal women with advanced breast cancer. Drugs 59(6):1279–1296

Corrigan OI, Li X (2009) Quantifying drug release from PLGA nanoparticulates. Eur J Pharm Sci 37(3–4):477–485

Das M, Sahoo SK (2012) Folate decorated dual drug loaded nanoparticle: role of curcumin in enhancing therapeutic potential of nutlin-3a by reversing multidrug resistance. PLoS One 7(3):e32920

Derringer G, Suich R (1980) Simultaneous optimization of several response variables. J Quality Technol 12(4):214–219

Dowsett M (1998) Theoretical considerations for the ideal aromatase inhibitor. Breast Cancer Res Treat 49(Suppl 1):S39–S44, discussion S73-37

Dubernet C (1995) Thermoanalysis of microspheres. Thermochim Acta 248:259–269

Feng S, Huang G (2001) Effects of emulsifiers on the controlled release of paclitaxel (Taxol) from nanospheres of biodegradable polymers. J Control Release 71(1):53–69

Fessi H, Puisieux F, Devissaguet JP, Ammoury N, Benita S (1989) Nanocapsule formation by interfacial polymer deposition following solvent displacement. Int J Pharm 55(1):R1–R4

Fonseca C, Simoes S, Gaspar R (2002) Paclitaxel-loaded PLGA nanoparticles: preparation, physicochemical characterization and in vitro anti-tumoral activity. J Control Release 83(2):273–286

George Box DB (1960) Some new three level designs for the study of quantitative variables. Technometrics 2:455–475

Henderson IC, Canellos GP (1980) Cancer of the breast: the past decade (first of two parts). N Engl J Med 302(1):17–30

Johannessen DC, Engan T, Di Salle E, Zurlo MG, Paolini J, Ornati G, Piscitelli G, Kvinnsland S, Lonning PE (1997) Endocrine and clinical effects of exemestane (PNU 155971), a novel steroidal aromatase inhibitor, in postmenopausal breast cancer patients: a phase I study. Clin Cancer Res 3(7):1101–1108

Joshi SA, Chavhan SS, Sawant KK (2010) Rivastigmine-loaded PLGA and PBCA nanoparticles: preparation, optimization, characterization, in vitro and pharmacodynamic studies. Eur J Pharm Biopharm 76(2):189–199

Kashi TS, Eskandarion S, Esfandyari-Manesh M, Marashi SM, Samadi N, Fatemi SM, Atyabi F, Eshraghi S, Dinarvand R (2012)

Improved drug loading and antibacterial activity of minocycline-loaded PLGA nanoparticles prepared by solid/oil/water ion pairing method. Int J Nanomedicine 7:221–234

Lam CX, Savalani MM, Teoh SH, Hutmacher DW (2008) Dynamics of in vitro polymer degradation of polycaprolactone-based scaffolds: accelerated versus simulated physiological conditions. Biomed Mater 3(3):034108

Lonning PE (1998) Pharmacological profiles of exemestane and formestane, steroidal aromatase inhibitors used for treatment of postmenopausal breast cancer. Breast Cancer Res Treat 49(Suppl 1):S45–S52, discussion S73-47

Mainardes RM, Evangelista RC (2005) Praziquantel-loaded PLGA nanoparticles: preparation and characterization. J Microencapsul 22(1):13–24

Mak KWY, Yap MGS, Teo WK (1995) Formulation and optimization of two culture media for the production of tumour necrosis factor-β in *Escherichia coli*. J Chem Technol Biotechnol 62(3):289–294

McPherson K, Steel CM, Dixon JM (2000) ABC of breast diseases. Breast cancer-epidemiology, risk factors, and genetics. BMJ 321(7261):624–628

Mehta AK, Yadav KS, Sawant KK (2007) Nimodipine loaded PLGA nanoparticles: formulation optimization using factorial design, characterization and in vitro evaluation. Curr Drug Deliv 4(3):185–193

Mendes GD, Hamamoto D, Ilha J, Pereira Ados S, De Nucci G (2007) Anastrozole quantification in human plasma by high-performance liquid chromatography coupled to photospray tandem mass spectrometry applied to pharmacokinetic studies. J Chromatogr B Analyt Technol Biomed Life Sci 850(1–2):553–559

Misra R, Sahoo SK (2010) Intracellular trafficking of nuclear localization signal conjugated nanoparticles for cancer therapy. Eur J Pharm Sci 39(1–3):152–163

Montgomery DC (2004) Introduction to factorial designs. Design and analysis of experiments. Wiley, New York

Moraes CM, de Matos AP, de Paula E, Rosa AH, Fraceto LF (2009) Benzocaine loaded biodegradable poly-(d,l-lactide-co-glycolide) nanocapsules: factorial design and characterization. Mat Sci Engi B 165(3):243–246

Musumeci T, Ventura CA, Giannone I, Ruozi B, Montenegro L, Pignatello R, Puglisi G (2006) PLA/PLGA nanoparticles for sustained release of docetaxel. Int J Pharm 325(1–2):172–179

Myer RH, Khuri AI, Carter WH (1989) Response surface methodology: 1966–1988. Technometrics 31:137–157

Myer RH, Montogomery DC (2002) Response surface methodology: process and product optimization using designed experiment, 2nd edn. Wiley, New York

Orozco-Castellanos LM, Marcos-Fernández A, Martínez-Richa A (2011) Hydrolytic degradation of poly(ε-caprolactone) with different end groups and poly(ε-caprolactone-co-γ-butyrolactone): characterization and kinetics of hydrocortisone delivery. Polym Adv Technol 22(4):430–436

Paolicelli P, Prego C, Sanchez A, Alonso MJ (2010) Surface-modified PLGA-based nanoparticles that can efficiently associate and deliver virus-like particles. Nanomedicine 5(6):843–853

Peppas NA (1985) Analysis of Fickian and non-Fickian drug release from polymers. Pharm Acta Helv 60(4):110–111

Zhang Q, Xu W, Wang Z (1994) Synthesis of polycaprolactone with two carboxy end groups. J Mat Sci Technol 10:351–354

Quintanar-Guerrero D, Allemann E, Fessi H, Doelker E (1998) Preparation techniques and mechanisms of formation of biodegradable nanoparticles from preformed polymers. Drug Dev Ind Pharm 24(12):1113–1128

Rahman Z, Zidan AS, Khan MA (2010) Non-destructive methods of characterization of risperidone solid lipid nanoparticles. Eur J Pharm Biopharm 76(1):127–137

Ray S (2006) RSM: a statistical tool for process optimization. Ind Tex J 117:24–30

Ray S, Lalman JA, Biswas N (2009) Using the Box–Behnken technique to statistically model phenol photocatalytic degradation by titanium dioxide nanoparticles. Chem Eng J 150(1):15–24

Redhead HM, Davis SS, Illum L (2001) Drug delivery in poly(lactide-co-glycolide) nanoparticles surface modified with poloxamer 407 and poloxamine 908: in vitro characterisation and in vivo evaluation. J Control Rel 70(3):353–363

Scott LJ, Wiseman LR (1999) Exemestane. Drugs 58(4):675–680, discussion 681–672

Seju U, Kumar A, Sawant KK (2011) Development and evaluation of olanzapine-loaded PLGA nanoparticles for nose-to-brain delivery: In vitro and in vivo studies. Acta Biomater 7(12):4169–4176

Seth AK, Misra A (2002) Mathematical modelling of preparation of acyclovir liposomes: reverse phase evaporation method. J Pharm Pharm Sci 5(3):285–291

Shah N, Chaudhari K, Dantuluri P, Murthy RS, Das S (2009) Paclitaxel-loaded PLGA nanoparticles surface modified with transferrin and Pluronic((R))P85, an in vitro cell line and in vivo biodistribution studies on rat model. J Drug Target 17(7):533–542

Strassmer-Weippl K, Goss PE (2003) Prevention of breast cancer using SERMs and aromatase inhibitors. J Mammary Gland Biol Neoplasia 8(1):5–18

Theobald AJ (2000) Management of advanced breast cancer with endocrine therapy: the role of the primary healthcare team. Int J Clin Pract 54(10):665–669

Thode K, Muller RH, Kresse M (2000) Two-time window and multiangle photon correlation spectroscopy size and zeta potential analysis—highly sensitive rapid assay for dispersion stability. J Pharm Sci 89(10):1317–1324

Yadav KS, Sawant KK (2010) Modified nanoprecipitation method for preparation of cytarabine-loaded PLGA nanoparticles. AAPS PharmSciTech 11(3):1456–1465

Yallapu MM, Gupta BK, Jaggi M, Chauhan SC (2010) Fabrication of curcumin encapsulated PLGA nanoparticles for improved therapeutic effects in metastatic cancer cells. J Colloid Interface Sci 351(1):19–29

Yang SC, Lu LF, Cai Y, Zhu JB, Liang BW, Yang CZ (1999) Body distribution in mice of intravenously injected camptothecin solid lipid nanoparticles and targeting effect on brain. J Control Release 59(3):299–307

Yee L, Blanch HW (1993) Defined media optimization for growth of recombinant *Escherichia coli* X90. Biotechnol Bioeng 41(2):221–230